JUTE FABRIC REINFORCED UNPAVED ROAD DESIGN

Muhammed Humayun Kabir **Mohammad Zaltaria**
Mohammad Zoynul Abedin **Gour Pado Saha**

ABSTRACT

Analysis and design method of jute fabric reinforced unpaved roads on clay subgrade is presented. Newly developed constitutive relations for two grades of jute fabrics and a silty clay subgrade soil is established. Design charts, appropriate for both the grades of jute fabrics, considering loadings from trucks, minibuses and light Cross Country vehicles (LCCV) are presented. Finally a design example is produced showing contribution from jute fabric reinforcing layer.

INTRODUCTION

Jute fabrics soaked in bitumen was used satisfactorily in unpaved road construction by the British in the Burma front during the second world war (SLIM, 1955), Since then there was no serious (reported) study on use of jute fabrics in road construction. In its present state jute fabrics with protective coatings may be used in construction of make shift roads for military and emergency uses. Research on durability and long term stability of jute fabrics would open use areas in permanent contstructions. Two grades of jute fabrics trade named CANVAS 36 X 16 and CBC 72 x 12 are included in this study. Repeated loading tensile tests were performed on both the grades and their mechanical behaviour were established according to a newly developed constitutive formulation (SAHA, 1988). The mechanical behaviour under repeated loading for a soft silty clay soil was also established using similar philosophy. A nonlinear design method, newly developed by SAHA and KABIR (1988), was used in developing design charts for both of the jute grades. These charts are appropriate for loadings from trucks, minibuses and Light Cross Country Vehicles (LCCV). To depict the philosophy a design example is produced, which is used to explain the corresponding load sharing mechanism.

Geometrical and loading condition

A typical cross section of an unpaved road is shown in Fig.l which also shows the geometry of the wheel contact areas. The geometrical and loading parameters appropriate for off highway trucks, minibuses and LCCV's are presented in Table 1.

The aggregates are assumed to be well graded, to provide sufficient interlock and effective load distribution. These should not have CBR (California Bearing Ratio) smallerthan 80.

For realistic representation of behaviour of clay soils, under repeated wheel loading , data from repeated loading undrained triaxlal tests Were used. Such tests were performed on representative samples under representative confining conditions. A new nonlinear constitutive formulation based on hyperbolic representation (KONDNER, 1963) was used to develop the e-$_c$-N relation and that for a silty clay, which is used in the designs presented here, may be expressed as follows :

$$\sigma = {}_{\varepsilon}\left[{}_{\sigma_1} - \log N / (C_1 + C_2 \log N) \right] \Big/ \left[(a_1 + C_3 \log N)\varepsilon_1 + (1 - a_1 - C_3 \log N)\varepsilon \right]$$

Table I. Wheel Loading Parameters

Vehicle / Parameter	Truck	Minibus	LCCV
Axle (Wheel)	Dual	Dual	Single
e(m)	1.88	1.64	1.20
B(m)	0.427	0.353	0.190
L(m)	0.214	0.249	0.226
B xL (m^2)	0.0914	0.0879	0.0429
P(kN)	80	60	24
Pc (kPa)	620	480	280

Table II. Properties of Jute Grades

Jute Grade / Parameter	Canvas 36x16	CBC 72x12
Weight (gsm)	540	370
Thickness (mm)	1.30	1.41
Pr_t (kN/m)	8.00	7.44
c_{rl} (10^{-2})	4.89	3.45
b_r (10^{-1})	2.53	2.50
r_1(10^{-3})	1.315	2.358
r_2(10^{-2})	0.00	2.285

Properties of constituent materials

Where, σ_1 = 40 kPa, ε_1 = 0.2 and a_1= 0.198 are limiting values and C_1= 0.105Kpa[1], C_2 = 0.1098 kPa^{-1} and C_3 = 0.02228 are calibration factors. The σ -ε-N relations for the clay, obtained from tests and from $_{\varepsilon}$q-l, are presented in fig. 2(a) showingfgood agreement.

As jute fabrics exhibit nonlinearity under wide ranges of strain levels, nonlinear load (Pr)-strain ( ) -number of load repeatations (N) relations similar to those suggested for clays were also developed using hyperbolic representation. Testing technique similar to that suggested by ANDRAWES, McGOWN and KABIR (1984), with slight modification for performing tests imder repeated loading, was adopted for this study (SAHA, 1988). Two grades of jute fabric were used in this study. The Pr - - N relations for both the grades may be represented as ,

$$P_{\varepsilon_{rl}}, -\varepsilon_{r1} - N$$

$$P_r = \left[P_{r1} \left(b_r + r_2 \log N \right)_{\varepsilon_r} \right] \Big/ \left[\left(\varepsilon_{r1} + {}_1 \log N \right) - \left(1 - b_r - r_2 \log N \right)_{\varepsilon_r} \right]$$

Where, and b_r are limiting values and r_1 and r_2 are calibration factors. Relevant values, along with some physical properties, for the two grades of jute fabrics are presented in Table II The , relations for both the grades of jute fabrics, from tests and from Eq.2 are presented in Figs 2(b) and 2(c), showing good agreement between them.

GIROUD and NOIRAY (1981) used two separate analyses, one is for very light traffic, the so called quasi static analysis, and the other for heavy traffic. In contrast the analyses, on which the proposed design method is based, use unified approach for any intensity of traffic loading.

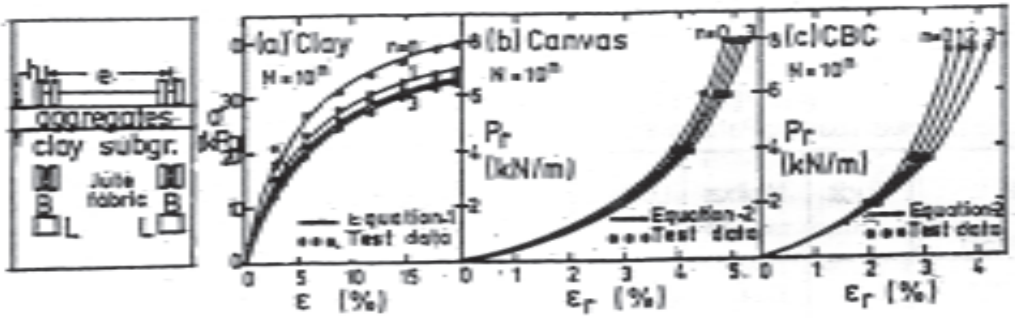

Fig. 1 Geometrical Description

Fig. 2 Mechanical Behaviour

Load distribution and geometry of deformation

A pyramidal distribution of load, from wheel, through the aggregate layer is assumed which is shown in **Fig.3**. The pres-sure at the base of the aggregate layer, may be expressed as (Fig.3),

$$p=p/[2(B+2h\tan\alpha)\,(L+2h\tan\alpha)]+\gamma h \qquad \ldots (3)$$

where, $\tan\alpha$ was taken as 0.60 as recommended by Giroud and Noiray. The wavy shape of the deformed unpaved road stretch results from incompressibility of the saturated clay subgrade. Schematic diagram of a road structure is presented in **Fig.4.** The relationships amongst the geo-metrical parameters are also shown on this , where, r is rut depth.

Design equations

The method of. development of design equations has-been described elaborately by Saha and Kabir. Tn this analysis, like that by Giroud and Noiray, the pressure relieving effect of the reinforcement is only considered.

The soil confining effect is not considered here. This will be reported in a forthcoming paper. From equilibrium consideration, the pressure, P, transmitted from the wheels through the aggregates on part AB (Fig.4) of the reinforced road should be equal to.

$$p = ps + pr \qquad \ldots . (4)$$

where, ps and pr are mobilised reac-tions (pressure) in the clay subgrade and the reinforcement respectively, appropriate for the intensity of traffic loading (N), un-der the same degree of rutting (Saha and Kabir). These mobilise reactions may be rep-resented as,

$$ps = \delta / (sl + s2\, d) + \gamma h \qquad \ldots (5)$$

$$\ldots (6)$$

$$b_r \equiv \left[\left\{(4+r_1(\log N)^2)/[P_{r1}(6+r_1(\log N))]\right\}\left\{1+16\delta^2\right)^{1/2}\right\}-2\Big]\Big/2$$

$$\varepsilon_r = \left[\left\{1+16\delta^2\right)^{1/2}\right\}-1\Big]\Big/2$$

Eq.5 is obtained by using an analytical scheme presented by PRAKASH, SHARAN and SARAN (1984). The pressure (ps) versus dimensionless deformation (δ =s / 2a) relation is established as a unique curve, whose hyperbolic representation defines the two constants s_t and s_2. The normal and. hy-perbolic representations of ps versus δ relation as a function of N are presented in **Fig.5.**

In Eq. and $(b_2 = (1-b_r - r_2 \log N)/[P_{rl}(b_r+r_2 \log N)]$

(Eq.2) and ε_r may be repre-sented as,

... (7)

Fig. 3 Pressure Distribution Fig. 4 Deformed Road Fig. 5 Ps - d Relation

ε_r may be expressed as a function of r and h by expressing d as a function of r and h. Again using Eqs.3,4,5 and 6 and tan $\alpha = 0.6$,

$$P/[2(B+1.2h)\,(L+1.2h)] = \delta/(S_1 + S_{2\delta}) + \{4/_{\varepsilon r}a(b_1+b_2\varepsilon_r)\}\ \{\delta^2/(1+16\delta^2)\}^{1/2} \qquad (8)$$

Design charts giving thickness of aggregated (h) as a function of rut depth (r) are produced for each of the grades of jute fab-rics. To facilitate checking of the strain level in the reinforcement the rut depth (r) versus reinforcement strain (C_r) as a function of aggregate thickness (j) are also produced. These charts for CANVAS, appropriate for loadings from trucks, minibuses and LCCV's are presented in Figs. 6(a), 6(b) and 6(c) respectively. Those appropriate for CBC are presented in figs 7 (a), 7(b) and 7(c).

Design Example, Discussion and Conclusions

To show the applicability of the design method, the following example is produced. A reinforced unpaved road should be designed for a minibus with p=60 kN, P_c=480 kPa, N = 1000 passages and r=170 mm, on the clay subgrade, incorporating reinforcing element of the type of jute thick-ness of aggregate layer, h=0.55m . The strain level in the jute fabric, under this performance is obtained as 1.9%

The design approach presented here enables the designer to establish, the load-ing path as well as the amount of load shared by the reinforcement under traffic loading. To elaborate this point, on fig.8, is now plot-ted the imposed loading (pressure) of the reinforced road system **[Fig.8(a)]**, the load (pressure) shared by the clay **[Fig.8(b)]**, that shared by the reinforcement **[Fig.8(c)]** and the relative share by the reinforcement **[Fig.8(d]**. These show, the jute fabric reinforcement to provide very small amount of resistance, although it is seen to increase with rutting due to load repeatations. In an unpaved road structure, like other relatively weak geotextiles, jute fabrics like the one under consideration, will function domi-nantly as separators rather than reinforce-ments. The load strain behaviour of both the grades of woven jute fabrics show initial sag typical of large crimp fabrics geosynthetics, purposely constructed for reinforcement function, are usually made of flat tapes or strands. These show relatively high initial modulus due to minimum crimp effect. However, both the jute fabrics showed small loss in stiffness under repeated loading compared with woven polypropy-lene geosynthetics (Saha, Saha and Kabir). To improve the reinforcement function of weak geosynthetics and jute fabrics, re-search on use of prestreched and prerutted reinforcements in unpaved road is under-way at the Bangladesh University of Engi-neering

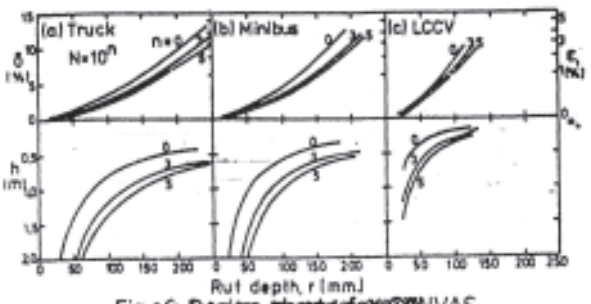

Fig. 6 Design charts for CANVAS

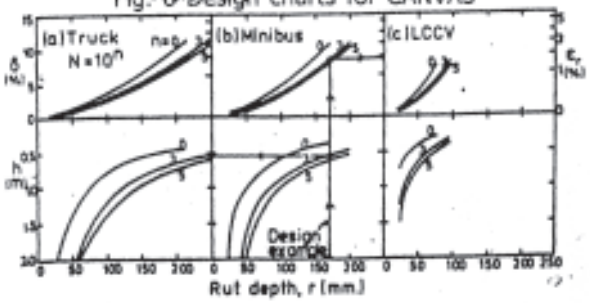

Fig. 7 Design Charts for CBC

On the basis of the work presented here, the following conclusions could be drawn. 1) Like other weak geosynthetics, the two grades of jute fabrics considered in this study show weak reinforcing effect. 2) The effect of crimp is high in case of woven jute fabrics constructed of round strands compared with their flat element geosynthetics counterparts. 3) Both the

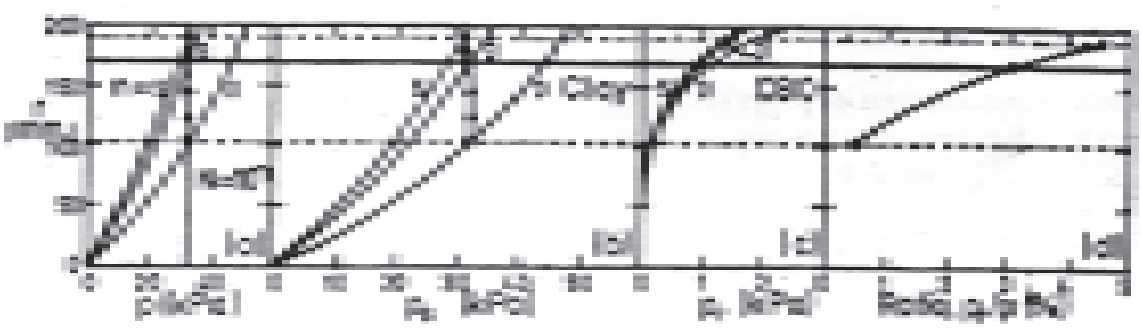

Fig.8 Load Sharing Mechanism

grades of jute fabrics show small loss of stiff-ness due to repeated loading compared with woven polypropylene geosynthetics. 4) The nonlinear constitutive relations, $\delta - \varepsilon - N$ for the clay and for both the grades of jute fabrics proved to be very satisfactory in fitting the test data. 5) Jute fabrics rein-forced unpaved roads will be suitable for transporting high volume of traffic within a short period of time.

REFERENCES

1. Andrawes, K. Z., McGown, A. and Kabir, M. H. (1984) : 'Uniaxial Strength Testing of Woven and Nonwoven Geotextiles', jour - Geotextiles and Geomembranes, Elsevier Applied Science Publishing, Vol. l,No. 1, pp. 41-56.
2. Giroud, J-P. and Noiray, L. (1981) : 'Geotextile Reinforced Unpaved Road Design', jour -Geotech. Engrg. Div,, ASCE, Vol. 107, GT9, pp. 1233-1254. $P_r - \varepsilon_r - N$
3. Kondner, R. L. (1963): Hyperbolic Stress Strain Response of Cohesive Soils', jour - Soil Mech. and Found. Div., ASCE,Vol - 89, SM3, pp. 115-143.
4. Saha, G. P. (1988) : 'Nonlinear Analysis and Design of Geotextile and Geogrid Reinforced Unpaved Roads', Forthcoming M. Sc. Engrg. The-sis, CE Dept. Bangladesh Univ, of Engrg. &Tech., Dhaka, Bangladesh.
5. Saha, G. P. and Kabir, M. H (1988): 'Design of Geotextile and Geogrid Reinforced Unpaved Roads', To be Published in the proc. of the Symp. on Theory and Practice of Earth Reinf. IS Kyushu, Fukuoka, Japan.
6. Slim, W. J. (1955): 'Defeat into Victory', War Memories, World War II.

APPLICATION OF JUTE GEOTEXTILE IN IMPROVING PERMEABILITY OF SUB SOIL

Satyendra Mittal, P. K. Choudhury, T. Sanyal and B. Chandrashekhar

ABSTRACT

The paper discusses the application of jute geotextile in improving the performance of weak sub soil based on the laboratory investigations. The permeability test and unconfined compression tests have been carried out by authors in order to study the effectiveness of jute geotextile. The results indicate that the permeability of soil increases with the use of jute geotextile and unconfined compression tests show that stress strain characteristics of black cotton soil are considerably improved with jute geotextile.

1.0 INTRODUCTION

Jute, a natural fibre, has traditionally been in use as a sacking material in India as well as in abroad. The versatility of jute fabric has made it possible to meet the technical requirements in the field of Geotechnical Engineering. Fabrics made of jute were tried in Dundee, Scotland (Kings way Road construction) in 1920s and in Kolkata, India (Strand Road construction) in 1934 with success long before the concept of man-made geotextile emerged. Jute mesh was also used for erosion control and side slope protection in the highways at United States in early 1930s. The U.S.A. started using open wave Jute Geotextile principally for slope erosion control and till date it is popularly used for the same purpose. The Bureau of Indian Standards has also published guidelines on the above use (IS-14986-2001).

Jute is produced mostly in Bangladesh, India and also in China, Thailand and Indonesia. Jute plant usually grows upto a height of about 3m with diameter varying between 20 to 30 mm. The bast fibres in the periphery of the plant are held together by sticky resin when harvested. The matured plants are cut, tied into bundles and kept submerged in water for about 20 days for retting. Fibres are then extracted from stems, washed in clean water, dried in the sun and sent to mills. The fibres thus obtained are processed mechanically in the jute mills to make yarn of the required diameter and tensile strength. These yarns are then woven into fabric with desired physical , mechanical and hydraulic properties suitable for different geotechnical applications. The existing machinery of the jute mills can also produce non woven jute geotextiles. Today, the Indian jute industries are well equipped to manufacture any type of site specific jute geotextile to cater to geotechnical requirements. India, with its varied topography has different types of soils like black cotton soils, organic soils, peats, clays, sand apart from soils in marshy lands and water logged areas. The pavement construction in these roads has always been problematic since the bearing capacity of such soils is low. In this regard, some techniques like stabilizing the sub-grade layer with soil cement mixes, lime plus flyash etc. have been suggested in the past. But stabilization requires selection of this proper material. A laboratory study has been carried out at IIT Roorkee, India with the support of JMDC and IJIRA to find the effectiveness of jute geotextile in improving the engineering properties of weak soil. The earlier studies indicate that Jute Geotextile appeared to provide effective solution and has gained gradual acceptance in applications in embankments, road pavements, earthen dam, retaining walls, hill slopes, river bank protection etc. worldwide.

2.0 MATERIAL USED

2.1 Soil Used

Sand, Black cotton soil and flyash have been used in the study. The engineering properties of these soils are given in Tables 1, 2 and 3 respectively.

Table 1 : Properties of sand used

1. Physical properties	
Specific gravity	2.58
2. Textural classification	
Gravel (%)	0.0
Sand (%)	97.6
Fines (%)	2.4
Textural classification	SP
3. Engineering properties	
OMC (%)	10.2
Dry density (t/m^3)	1.82

Table 2 : Properties of Black cotton soil used

1. Physical properties	
Liquid limit (%)	61
Plastic limit (%)	28
Shrinkage limit (%)	12
2. Swell index (%)	26.08
3. OMC (%)	21.6
4. MDD (t/m^3)	1.59
5. Soil classification	CH

Table 3 : Properties of Flyash used

1.	Grain Size Analysis	
	Sand Silt Clay	79.50% 20.17% 0.33%
2.	Classification	SM
3.	Liquid limit, Plastic limit	Nil
4.	Specific gravity	2.25
5.	e_{max}	1.92
6.	e_{min}	0.73
7.	M.D.D.	16kN/m^3
8.	Optimum Moisture Content	28%
9.	Cohesion (C)	Nil
10.	Angle of shearing resistance	43°

2.2 Jute Geotextile

Jute Geotextile of two different varieties , viz. woven and non woven were used as the reinforcing material. The properties of jute geotextile used in the study are given in Table 4.

Table 4 : Properties of jute geotextile

Property	Woven	Non-Woven
Weight (gm/m^2)	760	1000
Thickness (mm)	2	8
Width (cm)	76	150
Permittivity (m/sec)	0.5	10^{-3}
Strength (warp x weft) (kN/m)	20x20	6x7
Strain at break (warp x weft)	10% x 10%	25% x 30%

Chemical treatment with copper compound, natural addititive and bitumen usually enhance the durability of jute geotextile. BIS specifications for woven and non weaven jute geotextile are also available in IS : 14715-2000.

3. TESTS CONDUCTED

3.1 Permeability test for poorly graded sand

In order to study the influence of jute geotextile on the permeability of poorly graded sand, the permeability test was carried out with variable-head method in the laboratory by taking the standard permeability mould with its diameter 100 mm and height as 127.3 mm by compacting soil sample in three layers, each layer was given 25 blows at its OMC. Two tests were carried out, e.g. one test was conducted without jute geotextile (only soil sample) and another test was carried out with jute geotextile. One layer of jute geotextile was introduced at its middle. The laboratory test results show that the permeability of sub soil with the use of jute geotextile increased by 2 times as compared to permeability without jute geotextile (JGT). The results are shown in Table 5.

Table 5 : Effect of JGT on permeability of poorly graded sand

Coefficient of permeability without JGT	5.31 x 10^{-4} cm/sec
Coefficient of permeability with JGT layer in centre	1.21 x 10^{-3} cm/sec

3.2 Permeability test for black cotton soil

In order to study the permeability of black cotton soil with jute geotextile and without it but in addition of 10% of flyash, the permeability tests were carried out in the laboratory with the standard permeability mould. The soil sample was compacted in three layers and jute geotextile was placed at middle of the soil sample. Each layer was compacted by 25 blows at its OMC. Back pressure applied was 2 kg/cm^2 for the saturation of the sample and left for 48 hrs. After saturation of the sample, permeability test was carried out with variable head method. Back pressure application to the sample is shown in **Figure 3.**

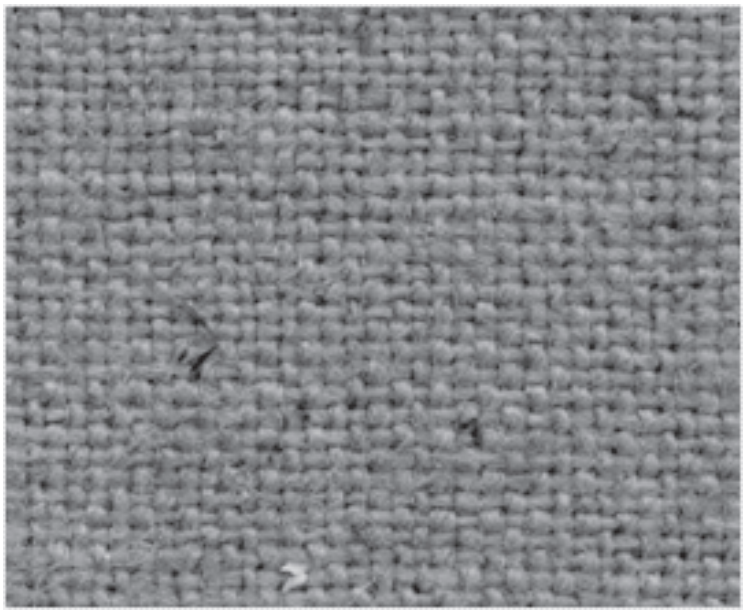

Fig. 1 woven type of Jute geotextile

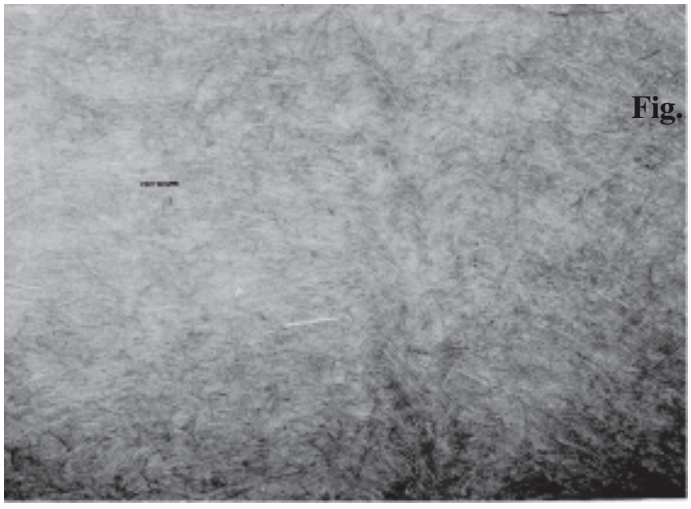

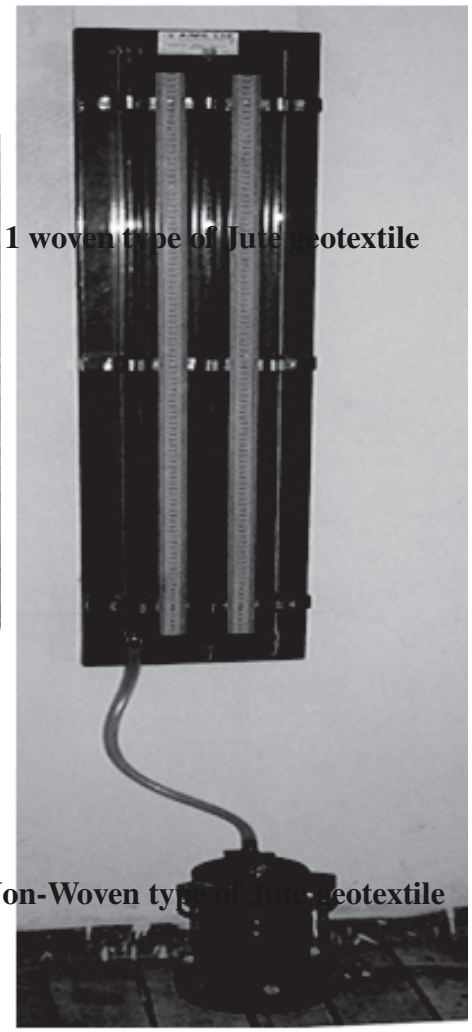

Fig. 2 Non-Woven type of Jute geotextile

Fig. 3 Bac

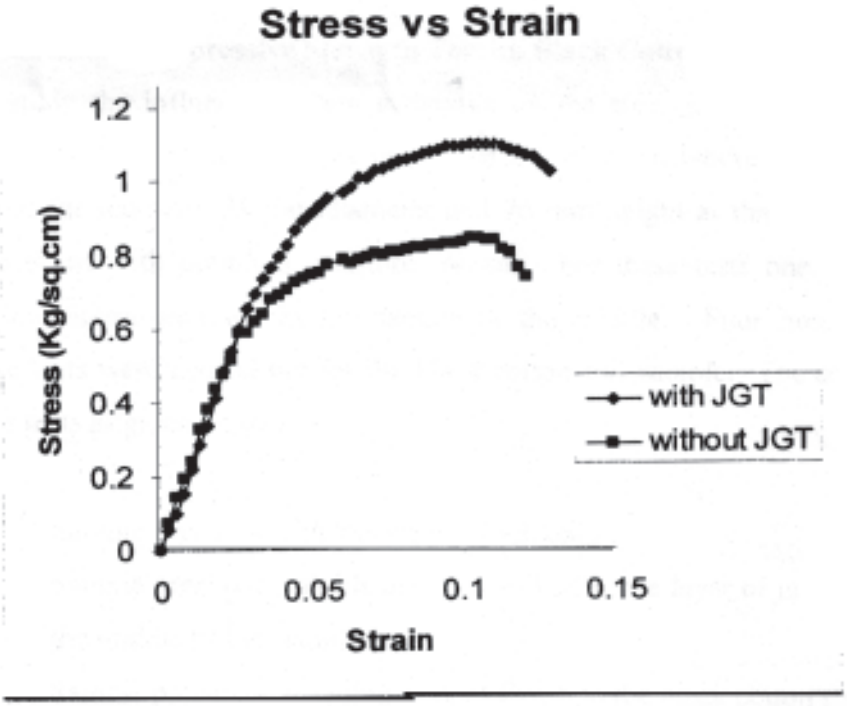

Fig.4 Effect of JGT on black cotton soil

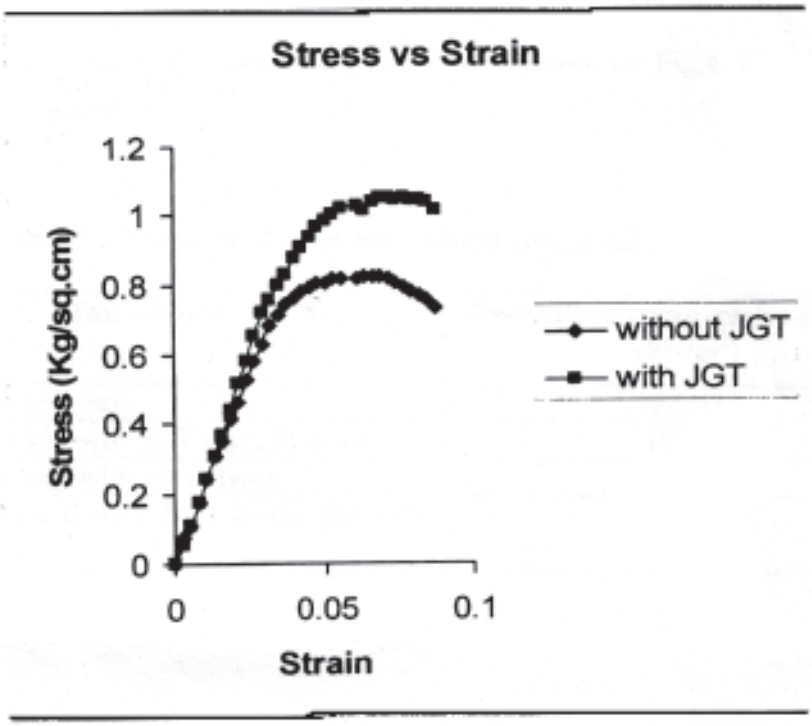

Fig. 5 Effect of JGT on black cotton soil with 10% flyash

Two permeability tests were carried out, e.g. one test was without jute geotextile in which only black cotton soil with 10% of flyash was used and another test was with jute geotextile in which one layer of jute geotextile was introduced in middle of sample. Test results are shown in Table 6.

Table 6 : Effect of JGT on permeability of black cotton soil with flyash

Coefficient of permeability for black cotton soil with addition of 10% of flyash by weight of black cotton soil, without JGT	04.6 x 10^{-8} cm/sec
Coefficient of permeability for black cotton soil with addition of 10% of flyash by weight of black cotton soil and with single layer of JGT in centre	2.74 x 10^{-7} cm/sec

It is evident from above results that permeability increases by 5 times when jute geotextile is used in the centre of soil specimen.

3.3 Unconfined Compressive Strength Test on Black Cotton Soil

To study the influence of jute geotextile on the strength of black cotton soil, unconfined compressive strength tests were carried out in the laboratory. The sample was prepared for test with 38 mm diameter and 76 mm height at the standard proctor compactive effort with optimum moisture content. For these tests one layer of jute geotextile was introduced within the sample at the middle. Four nos. unconfined compressive tests were carried out for the black cotton soil sample. The samples were prepared for tests as given below.

i) Sample prepared with black cotton soil only

ii) Sample prepared with black cotton soil with one layer of jute geotextile at the middle of the sample

iii) Sample prepared by adding 10% of flyash to the black cotton soil

iv) Sample prepared by adding 10% of flyash to the black cotton soil and one layer of jute geotextile at the middle of the sample

The results of unconfined compression tests are shown in Fig.4 and 5 and also summarized in Table 7.

Table 7 : Effect of JGT on unconfined compressive strength

Test sample	Unconfined compressive strength (kN/m^2)
Black cotton soil only	84.07
Black cotton soil with JGT layer in centre	109.63
Black cotton soil with 10% flyash	82.37
Black cotton soil with 10% flyash and JGT layer in centre	104.86

4.0 CONCLUSION

The results of the study are summarized as under -

i) Permeability of poorly graded sand with jute geotextile increases by **2 times** as compared to without jute geotextile.

ii) For black cotton soil with addition of 10% flyash by weight of black cotton soil, permeability with jute geotextile increases by **5 times** than without jute geotextile.

iii) The laboratory test results of unconfined compressive test show that stress strain characteristics of black cotton soil are better with jute geotextile than without it.

iv) Jute geotextile is much cheaper than man-made geotextile. Its strength properties are more or less comparable with synthetic geotextile.

v) Jute geotextile being eco-friendly holds an edge over its man-made counterparts.

It may thus be stated that jute geotextile can be used in improving geotechnical properties. Soil requires not only laboratory tests for qualification but necessitates field trials for corroboration of the laboratory results. The laboratory tests conducted on poorly graded sand and black cotton soil with jute geotextile to qualify the extent of improvement in soil permeability and unconfined compressive strength are pointers to the effectiveness of jute geotextile in soil improvement. Further tests are needed to the natural fabric's effectiveness in respect of other key soil parameters.

ACKNOWLEDGEMENT

The authors are thankful to JMDC and IJIRA, Kolkata for providing Jute Geotextile samples for conducting the research work.

REFERENCES

1. IS : 14715-2000 : "Woven Jute Geotextile specifications". Bureau of Indian Standards, New Delhi
2. Mehndiratta, H.C., Maruthi Sreedhar and Praveen Kumar (2002) : "Studies on durability of Jute Geotextile in embankments". Department of Civil Engineering, I.I.T. Roorkee (Uttaranchal).
3. Ramaswamy, S.D. and Aziz, M.A. (1989): "Jute Geotextile for Roads". Proc. Int. workshop on Geotextile, CBIP, Bangalore, Nov.,Vol. 1.1, pp 259-266.
4. Sanyal, T. & Choudhury, P. K. (2002) "Application of Jute Geotextile in Bank Protection Work in the Hugh Estuary - Appraisal of performance". Proc. "All India Seminar on application Jute Geotextile in Civil Engineering", Kolkata.
5. Jai Bhagwan, Yadav, 0. P. & Sharma, N. K. (2003) "Jute Geotextile for road applications - Field Trials". Proc. National Seminar on "Jute Geotextile an innovative jute products", New Delhi.
6. Sanyal T, Verma S. & Choudhury P. K. (2003) "Jute Geotextile in Slope Management - case studies in Sikkim & Meghalaya". Proc. "National Seminar on disaster management with specific reference to land slides and Avalanches", New Delhi.

INFLUENCE OF GEOJUTE REINFORCEMENT ON THICKNESS REDUCTION OF FLEXIBLE PAVEMENT - A MODEL STUDY

S. Chakrabarti, G. Bhandari

ABSTRACT :

The Geojute as horizontal reinforcement is beneficial in improvement of bearing capacity of sub-grade soil of low shearing strength and high compressibility; thus it is technically viable, cost effective alternative and environment friendly material. In the present investigation an attempt has been made to find out the behavioural changes of different pavement courses regarding bearing capacity and settlement on usage of Geojute (woven and non-woven), as horizontal reinforcement in the different interfaces of pavement courses of variable thickness in a flexible pavement. Model tests were carried out in the test pit of lmxlm area and 0.6 m depth. The thickness of each pavement courses was found out through field CBR test. The influence of Geojute reinforcement in reduction of the thickness of base course was observed by using Geojute at the interface of subbase and base course. The engineering properties of the different materials used including Geojute were found out in the laboratory, before the mode! tests.

1. INTRODUCTION

The subsoil of low shear strength and high compressibility is beneficial in improving the bearing capacity and settlement using soil reinforcement. The thickness of the pavement may be reduced, even in case of soft subgradc soil, using horizontal reinforcement at the interface of subgradc and subbase course or subbase and base course. Use of jute geotextile as reinforcement material in this regard is cost effective and technically viable, even though the jute is biodegradable in nature (Chakrabarty et al., 1997; Datta, 1998; Chakrabarti et al., 2002).

In the present investigation, an attempt has been made to find out the behavioural changes of different pavement courses regarding bearing capacity, settlement and corresponding reduction in thickness, on usage of Geojute as horizontal reinforcement in the different interfaces of pavement courses in a flexible pavement.

Model tests were carried out in the test pit of lmxlm area and 0.6m depth. The bottom of the test pit was considered as subgradc. The thickness of each pavement courses was found out through field CBR test. In the model test bottom ash, course aggregates and bituminous mix w ere used as subbase, base and surface course respectively. The influence of Geojute reinforcement in reduction of the thickness of base course was observed by using Geojute in the interface of subbase and base course (Haider, 1996).

The improvement of ultimate bearing capacity of the base course due to presence of Geojute was carried out through Plate Load (PL) test. Parametric study was carried out using different diameter of the Geojute at the interface of subbase and base course with varying depth of the base course. The improvement of bearing capacity of surface course due to presence of Geojute with varying diameter, as single layer reinforcement (at base-surface interface) as well as double layer reinforcement (at subbase-base and base- surface interfaces) was studied through PL test.

The engineering properties of the subgrade, subbase base and surface course materials including Geojute were found out in the laboratory before the model tests.

2. PROPERTIES OF THE MATERIALS USED

2.1 Subgrade Soil

The existing soil at bottom of the test pit was considered as subgrade material. The Optimum Moisture Content (OMC) of the subgrade was obtained as 40.30% and the corresponding dry density was 1.78 gm/cc, by Proctor Compaction test. The grain size distribution shows the material as silty sand in nature, where the silt fraction was 28.0%, while the fine sand and medium sand fractions were 54.0% and 18.0%. The undrained shear strength characteristics c_u and ϕ of subgrade were obtained as 3.5 t/m^2 and 24.5° respectively. The subgrade soil was found to be non-plastic in nature and the CBR value as obtained was 2.82%.

2.2 Bottom Ash

Bottom ash was collected from CESC, Gardenreach, Kolkata, which was used as the subbase material in the present investigation. Laboratory tests reveal that the material mainly comprises of the Oxides of Aluminium, Iron, Calcium and Magnesium. The OMC of used bottom ash was obtained as 30.13% and the corresponding dry density was 1.25 gm/cc. The grain size distribution was obtained as fine sand in nature in which the silt fraction was 8.4%, while the fine sand and medium sand fractions were obtained as 78.0% and 13.6% respectively. The shear strength parameters c and ϕ have 0.0 and 38° respectively.

2.3 Coarse Aggregates

The coarse aggregates of size 20mm down were used as base material over the subbase course. From the sieve analysis it was found that the coarse aggregate was well graded.

2.4 Bitumen

Hot bitumen was used to prepare the bituminous mix, which was used as surface course over the base course. Marshal stability test was carried out before bituminous mix design.

Marshal test was conducted in a cylindrical mould of 10.16cm diameter and 6.35cm height, with a base plate and collar. The mixed specimen was compressed radially at a constant rate of 5cm per minute and the maximum load, the specimen could withstand was 4.5% of coarse aggregate.

2.5 Geojute

Geojute was used at the different interfaces of pavement courses as horizontal reinforcement. Both woven and non-woven types were used in the model tests. The specifications of Geojute were as follows:

Woven Geojute: D.W. Canvass (87.5cm-16x 18-660gm/m^2) with a tensile strength 112kg/ 10cm in case of warp way and 120kg/10cm in case of weft way.

Non-woven Geojute: 7mm thick of weight 750gm/m^2, with a tensile strength 30kg/l0 cm in case of warp way and 35kg/ 10cm in case of weft way.

3. MODEL TESTS

The model tests were carried out in a test pit at field. The virgin soil at the bottom of test pit was considered as subgrade soil, the properties of which has already been described herein.

The different pavement course was then laid sequentially and each layer was compacted using 5.5kg rammer by controlling number of blows and height of fall, manually. Through

this manual compaction method the degree of compaction around 85% could be achieved and the degree of actual compaction was tested through sand replacement method. The sand pouring method was used to check the actual degree of compaction of different pavement course laid in the test pit. The complete pavement course consists of 170mm subbase using bottom ash on the subgrade soil; 127mm base course without Geojute, while 85mm in case of woven Geojute, and 100mm in case of non-woven Geojute, using coarse aggregates on subbase and finally 83mm surface course using bitumen (Halder, 1996).

The model tests were carried out in different conditions, which are as follows:

1) The entire pavement course without Geojute
2) Geojute placed at the interface of the base and subbase course
3) Geojute placed at the interface of the surface and base course
4) Geojute placed both at the interface of the surface and base course, as well as the base and subbase course
5) The tests for condition (2) through (4) was carried out using woven type Geojute and repeated for non-woven type Geojute.
6) Also the tests were carried out for different diameter ratio of Geojute with respect to diameter of plate in case of plate load tests.

The model tests include the field CBR tests and Plate Load tests, in different bed conditions.

3.1 Field CBR Tests

A pair of steel joists was placed parallel to each other, on the test pit, when the pavement course of different layers was ready. Then the field CBR machine was placed on these pair of steel joists, so that the central hole of the machine plate can be kept between these two joists. The plunger was passed through the central hole of the plate and kept it perpendicularly on the prepared test bed. Standard plunger of 5cm diameter was used for field CBR test. A proving ring and three dial gauges were attached to the machine with a standard arrangement for recording of gradually applied load and the corresponding settlement. Three dial gauges were attached to avoid the error due to uneven settlement. The average value of these three readings was considered for the estimation of settlement. The uplift pressure was resisted using block loads placed uniformly on the machine plate. The field CBR tests were carried out for the each layer of pavement course. According to the observed CBR values the construction depth of each pavement layer was found out using the standard CBR curves for flexible pavement design and subsequently the pavement thickness was then estimated.

3.2 Plate Load Tests

The similar arrangement except the plunger as used in field CBR tests, were used during the Plate Load tests. During Plate Load tests a load bearing plate of 12.7cm diameter were used. The tests were carried out on Flexible pavement without Geojute as well as with Geojute.

Plate Load tests on the model setup were carried out on the fallowings, in case of without Geojute. The thickness of the different courses were considered as per the field CBR tests and the degree of compaction as could achieved in the field:

1) Compacted subgrade soil
2) Upto subbase material laid on compacted subgrade. The subbase course was prepared at OMC and compacted upto 85%

3) Upto base course laid down on the compacted subbase course and subsequent course

4) On the completed surface course laid over the compacted base course and subsequent courses

The influences of Geojute layer on bearing capacity of different pavement course were also observed through Plate Load tests.

The size of the Geojute was considered as the diameter D, 2D, and 3D (D= Diameter of load bearing plate), which were placed at the single interface of base-subbase, base-surface or both interfaces. The diameter of Geojute was noted as D afterwards.

The stress corresponding to the settlement at 5% of diameter of the plate was considered as bearing capacity of the considered pavement course.

4. RESULTS AND DISCUSSIONS

The influences of Geojute layer in reduction of the thickness of base course was found through the field CBR tests, while the Plate Load tests were carried out on the different pavement courses to find out its stress-deformation characteristics and corresponding bearing capacity.

Table 1 shows the thickness of the pavement courses without Geojute at any interface and the corresponding reduction in pavement thickness when Geojute was in use at the interfaces.

Table 1

Thickness of the Pavement Courses

Pavement Course	CBRValue (%)	Depth of Const (mm)	Thickness (mm)
Subgrade	2.37	380	-
Subbase	6.74	210	170
Base: Type A	27.69	83	127
Base: Type B	17.50	125	85
Base: Type C	20.11	110	100
Surface	-	-	83

Base course has been categorised in three types, which are specified as Type A: without Geojute; Type B: with woven Geojute at the interface of subbase-base; Type C: with non-woven Geojute at the interface of subbase-base.

It is evident from Table 1, that the thickness of the pavement course was much less when woven type Geojute was in use at the interface of subbase-base, while it was moderate when non-woven type Geojute was used and high in case of without Geojute reinforcement support.

The Plate Load tests were carried out with different depth of base course, normalised to the diameter of the load bearing plate. Tables 2 through 5 are furnishing the changes in bearing capacity due to variation of normalised depth, influence of Geojute and diameter of Geojute normalised to the diameter of the load bearing plate.

Table 2

Influence of Woven Geojute at Subbase-Base Interface on Bearing Capacity

Bed Condition	Thickness of Base Course(Z)	Degree of Compaction (%)	Stress Ratio (σ_z/P)	Bearing Capacity (kg/cm*)
Without Geojute	0.50D	89.19	0.65	1.74
	0.75D	90.23	0.54	2.09
	1.00D	87.46	0.46	2.20
With Geojute (D'=D)	0.50D	87.26	0.65	1.93
	0.75D	88.14	0.54	2.36
	1.00D	86.28	0.46	2.66
With Geojute (D'=2D)	0.50D	86.12	0.65	2.31
	0.75D	85.06	0.54	2.91
	1.00D	88.26	0.46	3.12
With Geojute (D'=3D)	0.50D	89.42	0.65	3.03
	0.75D	88.13	0.54	3.78
	1.00D	86.48	0.46	4.14

Table 3

Influence of Non-woven Geojute at Subbase-Base Interface on Bearing Capacity

Bed Condition	Thickness of Base Course(Z)	Degree of Compaction(%)	Stress Ratio (σ_zp)	Bearing Capacity (kg/cm^2)
Without Geojute	0.50D	89.19	0.65	1.74
	0.75D	90.23	0.54	2.09
	1.00D	87.46	0.46	2.20
With Geojute (D'=D)	0.50D	88.72	0.65	1.88
	0.75D	86.06	0.54	2.30
	1.00D	86.74	0.46	2.59
With Geojute (D'=2D)	0.50D	88.62	0.65	2.10
	0.75D	88.01	0.54	2.70
	1.00D	87.68	0.46	2.94
With Geojute (D'=3D)	0.50D	86.46	0.65	2.50
	0.75D	88.10	0.54	3.23
	1.00D	89.64	0.46	3.64

Tables 2 and 3 reveals that the bearing capacity increases with the increase of normalised diameter of Geojute, how ever, it shows higher value in case of woven Geojute reinforcement than the non-woven. The degree of compaction may effect on the bearing capacity estimation through model tests. Repetitive tests are required with varying degree of compaction keeping the other parameters constant.

Tables 4 and 5 represent the improvement in bearing capacity due to single as well double layered reinforcement, with the variation of diameter of reinforcement. The tables reveal that the bearing capacity improves with the increase of the diameter of the reinforcement as well as, the number of layer. However, the improvement is higher in case of woven type than in the non-woven type.

Table 4

Influence on Bearing Capacity due to Single and Double Reinforcement using Woven Geojute

Bed System	Degree of Compaction(%)	Stress Ratio (σ_z/p)	BearingCapacity (kg/cm^2)
Without Geojute	89.43	0.50	2.80
Reinforcement at base-surface interface			
D'=D	90.42	0.05	3.40
D'=2D	88.79	0.05	4.09
D'=3D	88.48	0.05	5.02
Reinforcement at subbase-base & base-surface interface			
D'=D	89.64	0.5	4.96
D'=2D	90.02	0.5	5.38
D'=3D	89.62	0.5	6.24

Table 5

Influence on Bearing Capacity due to Single and Double Reinforcement using Non-woven Geojute

Bed System	Degree of Compaction(%)	Stress Ratio (σ_z/p)	BearingCapacity (kg/cm^2)
Without Geojute	89.43	0.50	2.80
Reinforcement at base-surface interface			
D'=D	90.42	0.05	3.00
D'=2D	90.42	0.05	3.53
D'=3D	90.32	0.05	4.24
Reinforcement at subbase-base & base-surface interface			
D'=D	88.68	0.5	4.08
D'=2D	88.62	0.5	4.65
D'=3D	89.42	0.5	5.32

Table 6 BCR for Varying Base Course Thickness

Nonnalised Thickness of Base Course Z/D	Normalised Diameter of Geojute (D'/D)					
	1		2		3	
	WG*	NWG	WG	NWG	WG	NWG
0.50	1.11	1.08	1.32	1.21	1.74	1.74
0.75	1.13	1.10	1.39	1.29	1.81	1.58
1.00	1.21	1.18	1.42	1.34	1.89	1.69

* WG = Woven Geojute; NWG- Non-woven Geojute

The Bearing Capacity Ratio (BCR) defines the ratio of bearing capacity with reinforced condition to the non-reinforced condition. Table 6 represents the BCR with the variation of thickness of the base course, while Table 7 represents variation with the number of reinforced layers.

Table 7

BCR for Number of Reinforcement Layers

Reinforcement Layer	Normalised Diameter of Geojute(D'/D)					
	1		2		3	
	WG	NWG	WG	NWG	WG	NWG
Single (Base-surface)	1.21	1.07	1.46	1.26	1.79	1.51
Double(Base-surface & subbase-base)	1.77	1.46	1.92	1.66	2.23	1.90

The BCR shows that the improvement of bearing capacity is in the range 8% to 89% for single reinforcement system in various thickness of base course, while 7% to 123% in case of doubly reinforced. The result reveals that the degree compaction is one of the prime factors for obtaining comparable bearing capacity.

5. CONCLUSIONS

It was observed from the present study that the thickness of base course of flexible pavement might be reduced by 32% in case of woven Geojute, while 20% for non-woven. Improvement of bearing capacity is as low as 7% and as high as 123%, in different bed condition and reinforcement layers. Uniformity in degree of compaction should be confirmed during the model tests to have the precise results on bearing capacity improvement. Mathematical correlations may be drawn or repetitive model tests may be arranged in this regard.

REFERENCES

Chakrabarty, S., Bhandari, G. and Adak, N. (1997). Performance of Model Footing on Compacted PFA, Geojute Reinforcement Overlaying Soft Clay, *Workshop on Jute Geotextiles,* Organised by IJMA & JMDC, Kolkata.

Chakrabarti, S., Bhandari, G. and Datta, A. (2002). Biodegradation Effect of Jute Geotextile as Soil Reinforcement for Improvement of Load-Settlement Characteristics, In the Proceedings of IGC 2002, held during December 20-22, 2002, at Allahabad, Vol. I, pp. 187-190.

Datta, A. (1998). An Experimental Study on the Effect of Degradation of Geojute on Load-Settlement Behaviour of Soft Soil Through Model Test, MCE Thesis submitted to Jadavpur University, Kolkata.

Haider, S. (1996). Influence of Geojute Reinforced Bituminous Layer on Load Settlement Behaviour of Flexible Pavements Through Model Test, MCE Thesis submitted to Jadavpur University

DEVELOPMENT OF ASPHALT OVERLAY FABRIC FROM JUTE

(Ms) M. Ghosh, P. K. Banerjee and G. V. Rao

A jute woven fabric employing leno based construction was designed for developing an asphalt overlay fabric, suitable for low traffic roads. To assess the suitability of this product, pavement models embedded with this fabric were subjected to accelerated cyclic mechanical loading and also to extended hygral loading. For the purpose of comparison, similar tests were also conducted on pavement models without any embedded fabric and also on those embedded with commercial fabrics. The experiments reveal that the pavement models embedded with the leno based product perform far better than the others. As a result of further analysis it was found that the grid-like structure of the new construction as also openings of suitable size were primarily responsible for the observed superior behaviour.

Keywords : asphalt overlay fabric; reflection cracking; jute; asphalt concrete beam; leno weave; grid-like structure

INTRODUCTION

Asphalt concrete (AC) overlay, a layer of a mixture of stone aggregates and asphalt, is applied for rehabilitating deteriorated pavements. Employing asphalt overlay (A/O) fabrics between new AC overlay and cracked pavement during road rehabilitation is a well-established method among different preventive measures to avoid reflection cracking.

Lytton (1989) reported that asphaltic pavements are subjected to distress due to traffic loading that causes differential deflections in the underlying pavement layers, and also due to ambient temperature fluctuations that result in expansion or contraction of the sub-grade (compacted soil foundation) and of the pavement itself. According to Dempsey (2002), reflection cracking is one of the major distresses frequently occurring in AC overlay in which the existing cracking pattern from the old pavement propagates up into and through the new overlay.

The first generation A/O fabrics were spun-bonded or needle-punched thin non-woven structures made out of polypropylene (PP) or polyester (Barazone, 1990; Barry, 1985; Bernard & Dobrosielskli, 1996; Geotextile Product Data, 2002; Marienfeld & Smiley, 1994; Maurer & Malasheskie, 1989). This kind of structure after an asphaltic tack coat application could only serve as moisture-proof layer and thereby prevent weakening of internal pavement structure owing to water infiltration and ultimately delay reflection cracking to some minor extent. According to Lytton (1989), a properly constructed reinforcing geotextile, having higher modulus than that of the surrounding AC, can turn a reflection crack into a horizontal plane beneath the reinforcing layer and thus delay the crack propagation indefinitely. Grids are stiffer and have various aperture sizes for proper anchoring with the surrounding aggregates. Starting with PP and high density polyethylene (HDPE) biaxial grids, very stiff (i.e. high modulus) fibre glass (FG) grids, which are generally knitted, are now capturing the market as PP and HDPE grids have higher extension at break than that required for the application. But grids cannot provide proper moisture proofing layer upon tack coat application. Consequently, A/O material with composite structure, resulting out of a combination of a grid-like reinforcement structure and a thin non-woven layer, was developed (Austin & Gilchrist,

1996; Cowell, Walls, & Salmon, 1985; Geogrid Product Data, 2002; Justo, 1989; Komatsu, Kikuta, Tuji, & Muramatsu, 1998; Lugmayr, Tschegg, & Weissenböck, 2002; Molenaar & Nods, 1996; Rao et al., 1991).

From the developmental history of A/O fabrics, a transition can be observed in selection of raw materials and construction, from non-woven spun-bonded or needle-punched structure of common synthetic fibres like PP, polyester towards grids and composite structures made of high modulus fibres like Kevlar and fibre glass. But no standard A/O material made up of natural fibres has been produced although some of the natural fibres like jute, sisal, hemp, flax, ramie, etc. (Batra, 1998, pp. 551–553; Roy & Sur, 2003, p. 14, 19; Stout, 1988, p. 2, 28) have mechanical properties better in many respects than PP or polyester (Mather, 2005, p. 262). A natural fibre like jute is also known to have good adhesion with asphalt as evident from the widespread application of asphalt-impregnated jute fabric. Hence, it appears reasonable to propose that A/O fabrics can also be manufactured from jute which is relatively inexpensive and abundantly available in India, Bangladesh and some neighbouring countries.

A pavement needs a durable protection. A jute-based product may not last long enough when subjected to elements of nature due its bio-degradability. To this end, investigations carried out by Banerjee and Ghosh (2008) on mechanical behaviour of jute in asphaltic medium upon hygral treatment and enzyme treatment simulating microbial attack reveal that hygral treatment of even a 6-month period is ineffective in damaging the jute-asphalt interface and the encased jute because, asphalt acts as protector for jute against microbial attack.

Consequently, a 100% jute-based asphalt overlay (JAO) fabric of moderate capability suitable for low traffic roads has been developed and its in situ performance within pavement in preventing reflective crack propagation under accelerated cyclic mechanical loading simulating traffic load investigated. Additionally, its efficacy to retard crack propagation after hygral loading, has also been evaluated through similar accelerated cyclic mechanical loading tests.

METHODOLOGY

Methodology for preparation of JAO

Jute yarns are made of relatively thick fibres (1.67–2.22 tex), resulting in diameters ranging between 0.7 mm (8 lb or 275.6 tex) and 1.8 mm (64 lb or 2204.8 tex). Hence, when such thick yarns are woven into a plain or twill fabric, very high values of crimp in the threads are encountered. The resultant fabrics therefore exhibit high extensibility. However, a leno-based construction made of thick and strong standard warp threads and thin weft threads, bound together by thin doup warp threads and plain woven bands of thick and strong weft and thin warp yarns inserted at proper intervals between two leno portions, can yield a product exhibiting very marginal crimp in the load-bearing warp and weft ends. Such a construction **(Figure 1)** is proposed for the basic load-bearing grid. At proper intervals between these load-bearing threads, plain woven bands of much thinner warp and weft yarns can be incorporated for acquiring the required asphalt-absorbency.

To weave such kind of fabric, one would require two beams, one each for standard and ground threads while the criss-crossing doup threads can be drawn from a separate creel. Similarly, supply of two different types of weft thread and an adjustable take up mechanism for weaving alternate bands of plain and leno are also necessary for developing such a product. In the case of non-availability of such a loom, one can produce the grid and the absorbent fabric separately and subsequently sandwich the latter between twolayersofthe grid.

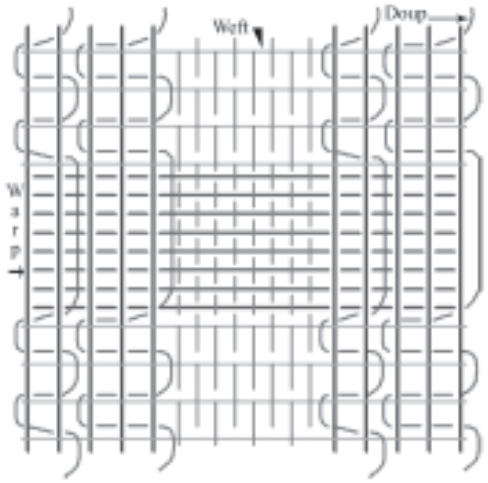

Figure 1. Structural construction of JAO.

Performance evaluation of JAO fabric

The evaluation of efficacy of JAO in retarding growth of reflection cracks due to mechanical and hygral loading was carried out by designing cyclic mechanical loading tests involving bending and shear strains. Such cyclic mechanical loading tests can be designed in two modes namely 3-point and 4-point bending. The shear stress and bending moment stress profiles under these two modes are essentially similar (Figures 2a and 2b) differing only around the central part of the beam. However, the shear stress changes the direction at the centre in the former case and is zero in the latter case, while the bending moment and hence deflection at the centre is higher in 3-point bending mode in the case of equivalent load application. Hence, 3-point bending mode was chosen for carrying out accelerated beam cyclic mechanical loading tests for evaluating the 'fracture properties' of the asphalt concrete beams (ACBs), with and without A/O fabrics.

The related research works of Lytton (1989), Brown, Thom, and Sanders (2001) and Cho, Kim, Lee, and Kim (2004) reveal that 3-point/4-point loading mode with point/semi-continuous support have been employed on geosynthetic material embedded ACBs by investigators to evaluate in situ performance of the A/O fabric. However, Brown et al. (2001) suggest that the 4-point loading with semi-continuous support simulates the field condition best. Hence, in the present study, a 3-point cyclic mechanical loading test programme with semi-continuous support was planned to carry out on ACBs using a suitable material testing system (MTS) where the frequency and amplitude of loading could be so varied as to impose a strain-rate well above that expected to be encountered on, for example a typical low traffic road, such as a district road in India.

To identify a combination of amplitude-frequency levels of mechanical loading that would result in reasonable number of loading cycles to failure from the view point of accuracy and test duration, an exploratory investigation was carried out on ACBs reinforced with a commercial asphalt-impregnated jute geotextile (JGT). This fabric has a moderately high modulus but does not exhibit any pronounced grid-like structure. This experimentation was based on a two-factor second-order central composite design. According to the experimental design adopted, JGT-reinforced ACBs were tested at 10 different factor-level combinations of load and frequency.

Based on the literature as also requirements of accelerated test, mechanical loading domain was selected as below :

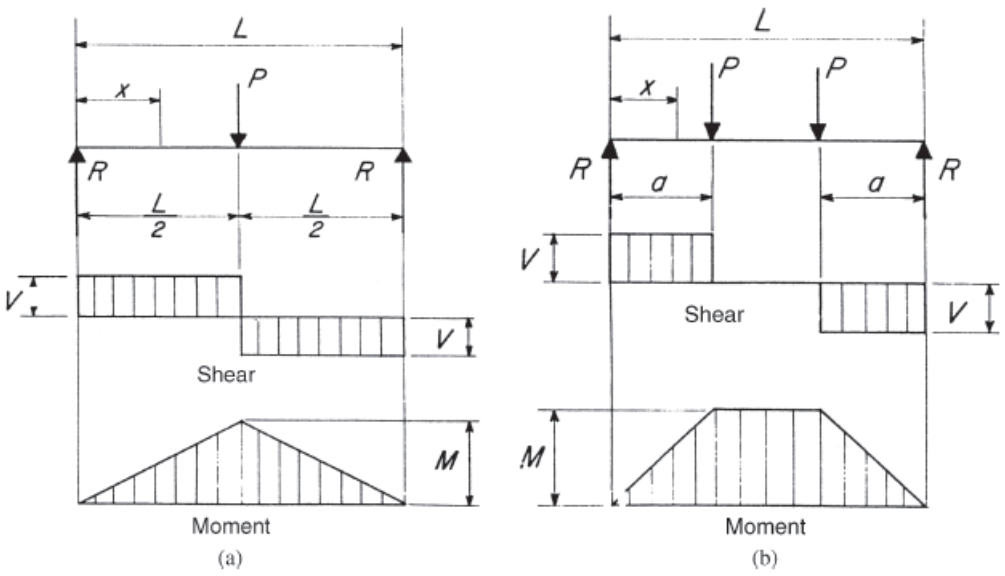

Figure 2. (a) Shear and bending stresses in a simple beam in 3-point bending mode. (b) Shear and bending stresses in a simple beam in 4-point bending mode.

- Range of amplitude of loading, Min.: 28.79% of breaking load of ACB in static loading, Max.: 71.21% of breaking load of ACB in static loading.
- Ratio of minimum to maximum load during a test cycle: 0.1.
- Range of frequency of loading: Min.: 10.76 Hz, Max.: 19.24 Hz.
- Nature of loading: Sinusoidal.

The performance of JAO-embedded ACB was tested employing the identified amplitude-frequency level combination. Simultaneously, unreinforced ACBs as well as those embedded with a commercial synthetic strain-relieving A/O fabric (PP non-woven paving fabric, code named SGT) were also tested under the same loading conditions to understand the effect of different types of A/O fabrics in prevention of crack propagation.

Unreinforced ACBs were also subjected to cyclic mechanical loading testing on MTS at five different loads under a moderate level of frequency.

The effect of hygral loading was studied on unreinforced ACBs and ACBs embedded with JGT, JAO and SGT. To this end, beam specimens were subjected additionally to two different levels of hygral treatment by immersion under water for 15 and 30 days, respectively. Subsequently, the ACBs were removed from water and subjected to the specific identified loading conditions obtained from the exploratory experimentation with JGT.

Experimental procedures

Preparation of JAO fabric

It was decided to initially aim at the following specifications for JAO fabric:

1. A breaking load in the region of 30 kN/m in both length and width directions.
2. A breaking elongation lower than 5% in both length and width directions.
3. Grids on fabric surface of opening size in the range of 15 mm.
4. Ability of absorbing asphalt and forming a continuous impermeable layer.

The materials and process sequence chosen for development of leno-weave-based JAO fabric samples were guided by the constraints imposed by the facilities of the departmental laboratory primarily catering to cotton system as also by the necessity of avoiding the sizing process.

Type of test	Size of test specimen (L × W)[a] (mm × mm)	Size of jaw faces (A × B)[b](mm × mm)	Gauge length (mm)	Rate of deformation (mm/min)
Grab	203.2 × 101.6	25 × 50	75	300
Wide-width	200 × 200	200 × 50	100	10

[a]L = length of specimen, W = width of specimen. [b]A = size of jaw faces perpendicular to the direction of load, B = size of jaw faces parallel to the direction of load.

Two types of commercial jute yarns were chosen for weaving the fabric. The stronger one (21.5 lb or 742 tex), meant for the standard threads, was 1.4 mm thick having a breaking strength of 94 N (CV = 13.7%) and a breaking extension of 3.3% (CV = 13.5%) while the thinner one (9.1 lb or 315 tex), meant for the doup and ground threads, was 0.75 mm thick having breaking strength of 32.7 N (CV = 19.5%) and 2.3% (CV = 12.1%) breaking extension.

For working out details of the sett of the fabric, it was initially assumed that the mean single yarn strength of the standard thread would be realised to the extent of 80% in the fabric. Keeping in view the effective reed width of 400 mm of the handloom on which the fabric was to be woven as also the necessity of keeping the fabric as thin as possible the following combination was derived:

1. Count of reed: 8 Stockport.
2. Number of standard threads in adjacent pairs of strand: 3 and 2.
3. Total number of pairs of strands of standard thread: 16.
4. Number of ground threads between two neighbouring pairs of strands of standard thread: 8.
5. Total number of doup threads: 32.

This fabric in folded form is expected to yield the desired strength in warp direction. The weft insertion sequence was designed appropriately so that 20 load-bearing threads could be accommodated in the fabric for each 100 mm length, interspersed with thinner ground threads at regular intervals.

Determination of tensile properties of fabrics

Grab tensile test (ASTM D 4632–86) and wide-width tensile test (ASTM D 4595–86) was carried out on the fabrics for finding out breaking load, elongation at break and Young's modulus. The conditions adopted for grab and wide-width tensile testing as per relevant ASTM standards were as shown above. The test results are shown in Table 1.

Evaluation of in situ performance of fabrics

(a) Preparation of ACBs

Asphalt concrete mix used for the present study was a dense bituminous (or asphaltic) macadam (DBM) mixture with an asphalt content of 5.5%. The composition of the DBM mixture is given in Table 2. The dimension of the ACBs was determined according to the particle size distribution of the aggregate mix. The maximum particle size of the main contributing section of the aggregate mix was 10 mm. The width and height of the ACBs would be 7.5 times of the maximum particle size and the length would be 3 times of width. So the ACBs, as shown in Figure 4, were prepared of dimension 225 mm (L)× 75 mm (W)× 75 mm (H). A transverse

notch of 5-mm depth and 3-mm base-width at the beam-centre was created to simulate a pre-existing crack in the old pavement. A/O fabric reinforcement was placed at 20 mm above the beam specimen-base for reinforced specimens.

Table 1 : Tensile properties of A/O fabrics.

		Breaking load (CV%)		Breaking elongation (CV%)		Young's modulus in MPa (CV%)	
Type of test	Type of sample	Warp-way	Weft-way	Warp-way	Weft-way	Warp-way	Weft-way
Grab	JAO (double layer)	0.98 kN	0.84 kN	9.4	9	104.9	96.1
		(10.2)	(10.9)	(7.1)	(5.6)	(8.9)	(9.3)
	JGT	1.2 kN	1.19 kN	6.6	8.7	183.5	324
		(3.5)	(8.4)	(6.8)	(8.4)	(17.1)	(13.8)
	SGT	0.56 kN	0.53 kN	88.2	71.8	28.4	37.2
		(17.3)	(11.4)	(11.7)	(14.5)	(12.5)	(6.8)
Wide-width	JAO (double layer)	24.2 kN/m	24.8 kN/m	5.1	4.9	79.6	107.0
		(14.1)	(3.3)	(13.4)	(6.8)	(7.7)	(14.0)
	JGT	25.6 kN/m	27.1 kN/m	2.9	4.9	343	263.9
		(3.2)	(3.3)	(12.9)	(14.1)	(19.4)	(15.7)

Table 2. Composition of dense graded bituminous macadam pavement layers.

Grading	2
Nominal aggregate size	25 mm
Layer thickness	50–75 mm
Indian Standards (IS) sieve (mm)	Cumulative% by weight of total aggregate passing
45	
37.5	100
26.5	90–100
19	71–95
13.2	56–80
9.5	—
4.75	38–54
2.36	28–42
1.18	—
0.6	—
0.3	7–21
0.15	—
0.075	2–8
Bitumen content% by mass of total mix[b]	Min. 4.5
Bitumen grade (pen)	65 or 90

[a] The combined aggregate grading shall not vary from the low limit on one sieve to the high limit on the adjacent sieve. [b]Determined by the Marshall method.

(b) Determination of breaking load of ACB under static condition.

For determining the breaking load of ACB with and without A/O fabric, under static loading condition, tests were conducted under 3-point bending mode using a loading frame. The deformation rate employed on ACB samples was 15 mm/min. From these tests, breaking load range of 1.08–1.47 kN was obtained and their average value was adopted as maximum load capacity of the ACBs.

(c) Hygral treatment of ACBs

In extreme condition of monsoon in India, some areas become flooded for two to three weeks at a stretch. Hence, for investigating the effect of hygral loading on the performance of ACBs, some samples were kept immersed in water for 15 and 30 days before subjecting them to cyclic mechanical loading tests. The three levels of hygral load thus were 'zero' time submerged under water (for simulating real-life situation in seasons other than monsoon), 15-day water-submerged and 30-day water-submerged (for simulating flooded road condition during extremes of monsoon).

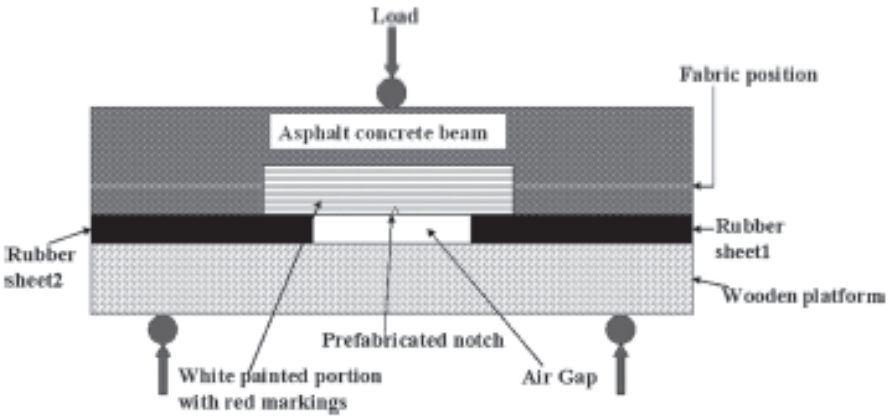

Figure 3. Schematic diagram of the experimental set-up for cyclic mechanical loading testing of ACBs.

(d) Cyclic mechanical loading test of ACBs

Cyclic mechanical loading test of ACBs were carried out on an MTS under 3-point bending mode with 'semicontinuous' support system. Before testing the ACBs on MTS, both the side surfaces of the beams were painted with white road-paint and marked with horizontal red lines at intervals of 5 mm up to 30 mm level above the beam-base to record the crack height with number of loading cycles during test.

The experimental set-up is shown in **Figure 3.** Support was provided by two 20-mm-thick layer of rubber pieces with a central gap of 50 mm and placed over a wooden base. This is to facilitate quick propagation of crack from and around the notch upwards in the event of a 3-point bending regime. The cyclic mechanical loading load was applied at the third point, as in a 3-point bending test.

The crack propagation (i.e. crack height) with number of loading cycles was recorded by taking photographs with the help of a 5-mega pixel digital camera. In order to achieve a degree of confidence in the experimental data, tests for each combination of mechanical and

hygral loading parameters were repeated and the average was chosen as the response value.

(e) Determination of extent of damage in the exhumed A/O samples

A/O fabric samples were exhumed from the ACBs by softening the beam through heat. Subsequently, the asphalt coated fabric samples were cleaned several times with petrol so that the damages were clearly visible. Photographs of cleaned and dried samples were taken for damage analysis.

Results and discussions

Tensile properties of JAO

The JAO (Figure 4) was folded back along its length and the double-layered product of effective areal density of 886.2 g/m^2 was tested by subjecting it to Grab and Wide-width tensile tests (Table 1).

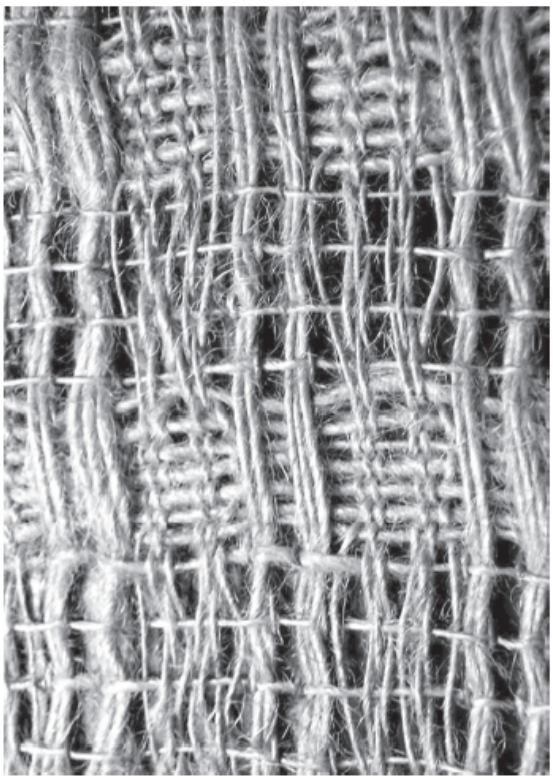

Figure 4. Actual photograph of JAO fabric (single layer).

The breaking strength values resulting out of grab test are much higher if one considers the same in terms of linear meter width, than those from the wide-width test results. This anomaly is partly caused by the lower gauge length in grab test permitting the jaws to grip more number of fibres of the constituent yarns at both ends, as the fibre length distribution in typical jute yarns shows a wide spectrum varying between few centimeters to nearly 30 cm. Moreover, the lower width of the jaw coupled with lower gauge length in grab test meant a much smaller yarn length (about one-fifth) under test at any time compared to that in wide-width test. This too effectively reduces the number of weak points considerably. Much higher deformation rate adopted in grab test as compared to wide-width test would also result in higher breaking strength value. Additionally, in grab test, the extra portions of the fabric

width beyond the jaws yield some additional fabric assistance.

While comparing the breaking strength, elongation and modulus values of JGT and JAO, it is observed that JGT is as strong as JAO while its stiffness is higher and elongation is lower. However, the asphalt-impregnated JGT has an areal density of 1515 g/m^2 as compared to that of JAO which is only 886.2 g/m^2. The structural superiority of JAO over JGT is thus clearly evident. The somewhat lower breaking elongation and considerably higher stiffness of JGT is also caused by the binding effect of asphalt, as has been reported elsewhere (Banerjee & Ghosh, 2008).

Nonetheless, there exists a considerable gap between the targeted values of strength in JAO and the value actually achieved. A view of JAO (Figure 4) reveals the cause. The load-bearing warp threads remain parallel to each other during the insertion of the load-bearing thick weft threads. However during the actual leno weaving, the criss-crossing doup threads roll the standard threads and deviate from their desired location in fabric. Hence, the load-bearing standard threads do not share the tensile load equally, when a fabric sample is tested for strength in warp direction. The load-bearing thick wefts too show considerable deviation from their desired straight and parallel location in the fabric, resulting in a similar fall in effective strength. Clearly, such defects have been caused primarily due to limitations on handloom related to the proper control of tension in the different warp and weft threads. The rolling caused by allocation of one doup thread to the strand of two or three standard threads also contributes to the lower strength and modulus than targeted at.

The grab test results of the strain-relieving SGT fabric reconfirm the low strength and high extensibility of this class of fabric.

Grid size

The fabric was woven in such a manner that the doup threads remained idle for eight cycles and was made to switch sides around the strands of standard ends for four cycles. During the eight cycles of plain weaving, the tension in the doup threads remained stable and the resultant grid created between pairs of columns of standard ends exhibit the range of 20–23 mm in length direction and 15–16 mm in width direction. However, during the subsequent four cycles, the tension in the doup threads rose sharply during the beating up process, creating openings within the two columns of strands as also between the neighbouring pairs of columns. The opening size created within the pairs of columns exhibit the range of 4–7 mm in length direction and 3–4 mm in the width direction.

Hence, the resultant fabric exhibits a distribution of grids between small ones measuring 4 mm × 4mmtolarge ones of 23 mm × 16 mm.

Performance of A/O fabrics in ACB under cyclic mechanical loading and hygral loading

Regression equations were derived from the experimental data obtained by testing the JGT-reinforced ACBs at 10 different factor-level combinations of load and frequency (Table 3), relating the number of cycles required for the crack to reach a particular height for a given combination of frequency and amplitude of loading. These equations, shown in Table 4, for number of cycles for crack to reach 20 mm (the height at which JGT is located), 25 mm and 30 mm height, yield coefficient of determination values of 0.741, 0.909 and 0.898, respectively. These values of the coefficient imply that the number of cycles required for crack to flow into the pavement layer above the JGT fabric is primarily determined by the amplitude and frequency of loading while the crack propagation up to the level of JGT is influenced by

other variables as well, such as the resistance offered by the JGT. The regression equations reveal that the effect of load is more dominant than that of frequency on the rate of crack propagation as in each case the coefficient associated with load factor is substantially higher than that of frequency. Plots of number of cycles required to reach 30 mm height from beam-base versus maximum peak load for five different frequencies were drawn using the regression equations **(Figure 5)**. These traces reveal that number of cycles required for a certain level of distress rapidly falls with increasing load but beyond a certain level of load the rate of fall becomes marginal. This critical load value as also the reduction in the rate of drop in the number of cycles for failure with increase in the load is attributed to the presence of A/O fabric. Apparently, a basic resistance is offered by this fabric towards growth of crack from the notch up to and just beyond the level at which it is embedded in the beam irrespective of the level of load and frequency of test. This influence is verified by the results of the experimental set with non-reinforced ACBs which show that the number of load cycles falls sharply with increase in load level without any change in the slope **(Figure 6)**.

Table 3. Different combinations of maximum peak load and frequency adopted for cyclic mechanical loading testing of JGT reinforced ACBs.

Actual value of maximum peak load (kN)	Coded value of maximum peak load, x	Actual value of frequency (Hz)	Coded value of frequency, y
0.42	-1	12	-1
0.42	-1	18	1
0.78	1	12	-1
0.78	1	18	1
0.34	-1.414	15	0
0.85	1.414	15	0
0.60	0	10.76	-1.414
0.60	0	19.24	1.414
0.60	0	15	0
0.60	0	15	0

Table 4 : Regression equations from cyclic mechanical loading testing of JGT-reinforced ACBs.

Crack height (mm)	Regression equation	Multiple R	Squared multiple R
20	Z = 826.781 - 1307.597*x - 529.358*y + 1078.829*x*x + 685.711*y*y + 651.75*y*x	0.861	0.741
25	Z = 1912.687 - 2420.348*x - 866.281*y + 1806.456*x*x + 314.005*y*y + 1352.25*y*x	0.953	0.909
30	Z = 5925.297 - 3650.424*x - 1820.596*y + 1929.988*x*x + 171.457*y*y + 295.5*y*x	0.948	0.898

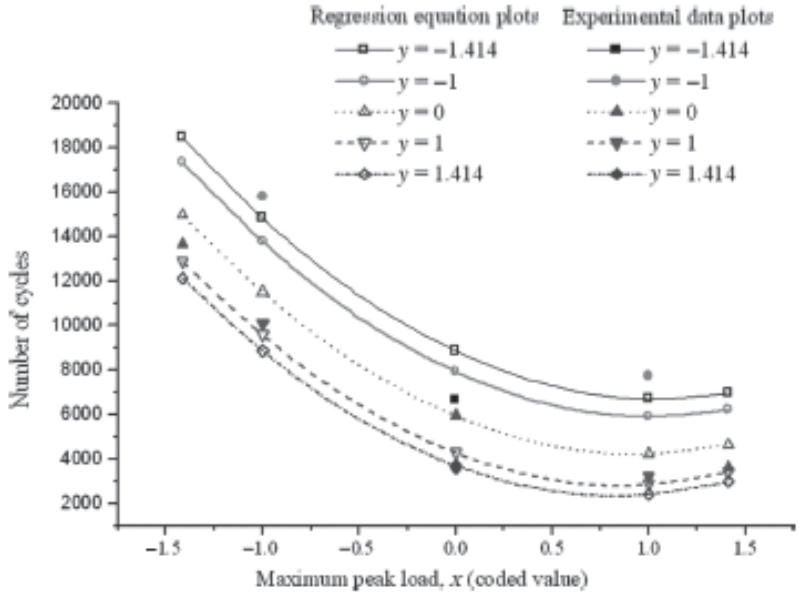

Figure 5 : Plots of number of loading cycles versus maximum load at different frequencies for JGT-reinforced ACBs

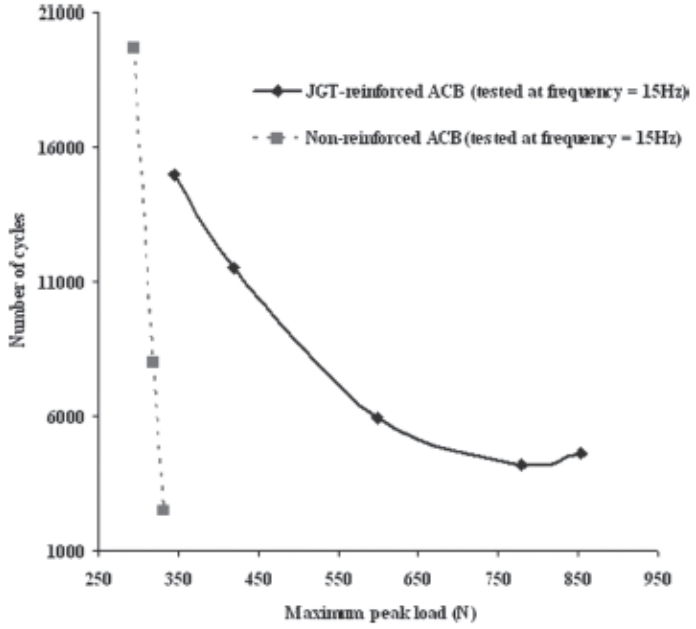

Figure 6. Effect of reinforcement in crack propagation within ACB.

For testing the efficacy of the JAO and SGT fabrics in ACB vis-`a-vis unreinforced ACBs, the load was kept at the critical value 1 (0.78 kN) achieved with JGT while a moderate frequency of 0 level (15 Hz) was chosen. This would permit a reasonable number of test cycles to failure, any change in the slope (Figure 6). both from the point of view of accuracy as also test duration.

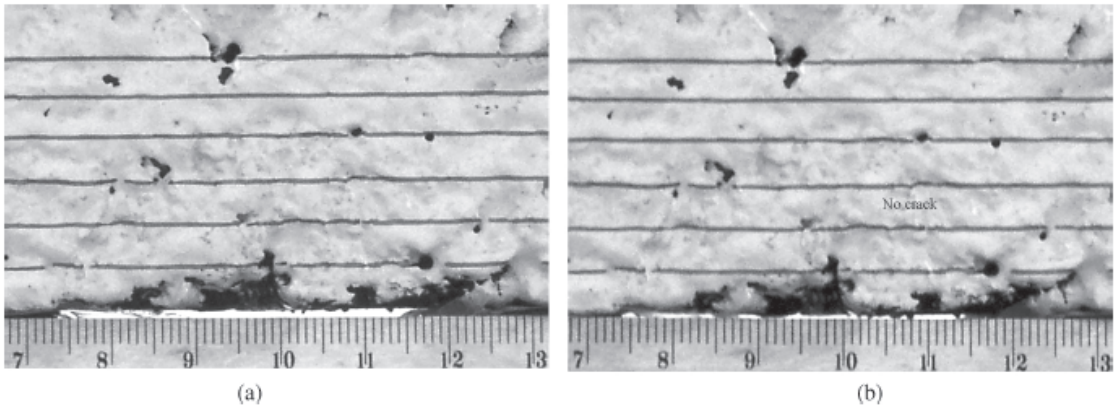

Figure 7. Front views of ACB with JAO embedment (a) before and (b) after cyclic mechanical loading, tested at maximum peak load = 0.78 kN, frequency = 15 Hz, number of cycles = 19865.

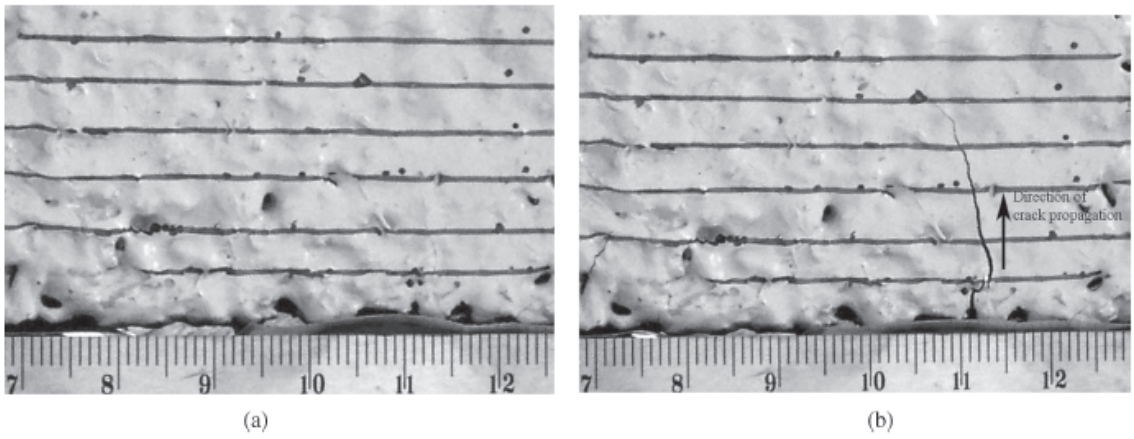

Figure 8. Front views of asphalt concrete beam with JGT embedment (a) before and (b) after cyclic mechanical loading, tested at maximum peak load = 0.85 kN, frequency = 15 Hz, number of cycles = 7483.

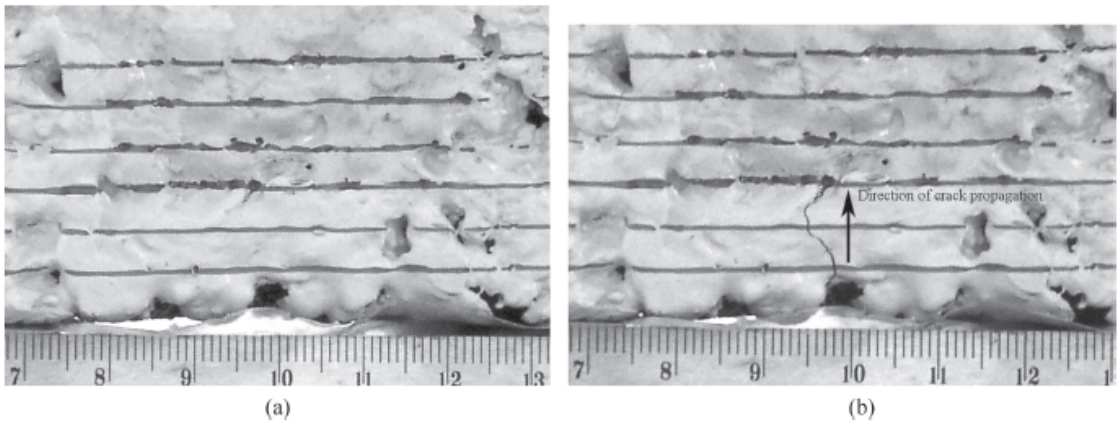

Figure 9. Front views of asphalt concrete beam with SGT embedment (a) before and (b) after cyclic mechanical loading, tested at maximum peak load = 0.78 kN, frequency = 15 Hz, number of cycles = 6297.

Experimental results reveal that under all experimental conditions, ACBs embedded with JAO do not exhibit any crack propagation beyond the level at which the JAO is placed within the ACB. Moreover, in many cases the crack initiated at the notch did not grow at all. A typical photograph of crack propagation in JAO-reinforced ACB **(Figure 7)** confirms this observation.

The ACBs embedded with JGT and SGT exhibited growth of crack well beyond the A/O layer (depicted in **Figures 8 and 9**). The JGT appears to delay this growth better than the SGT.

The experimental data pertaining to hygral loading of unreinforced ACBs exhibit a sharp drop in resistance to crack propagation after a 15-day immersion while the 30day immersed samples exhibit stiffening that matches that of the dry control sample. The JGT-reinforced ACBs exhibit a trend that shows continuous improvement in resistance to crack propagation with increasing duration of hygral loading. However, the JAO-reinforced ACBs show the best results indicating no development of crack whatsoever, both after 15-and 30-day immersion.

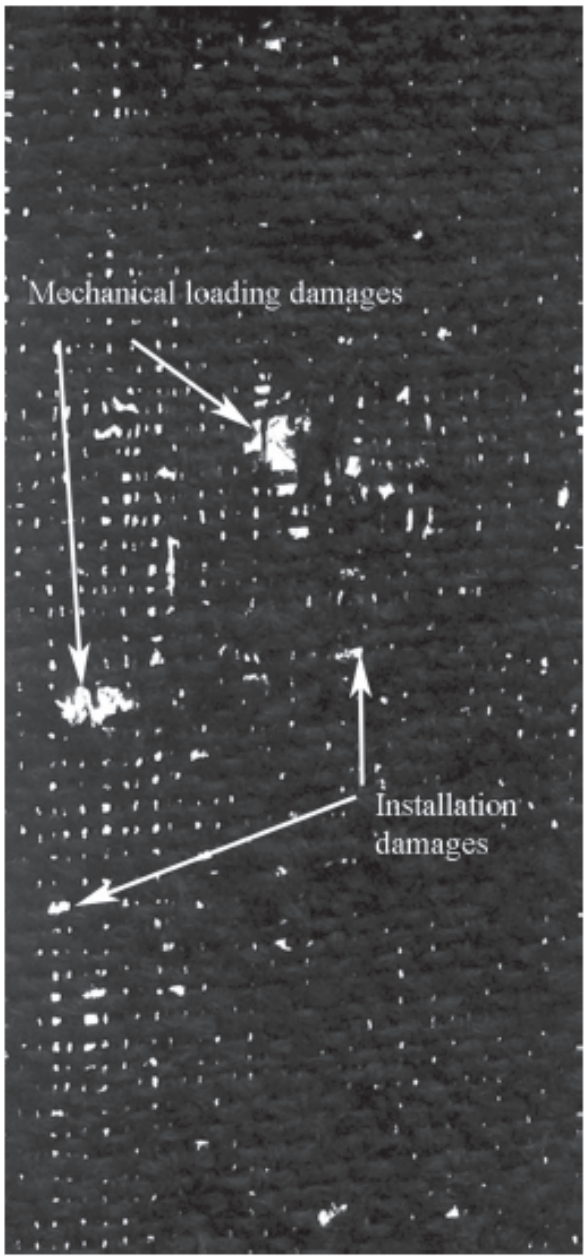

Figure 10. Exhumed JGT sample tested at maximum peak load = 0.78 kN, frequency = 18 Hz.

Studies on the exhumed A/O samples

On visual observation, the JGT sample **(Figure 10)** was found to have been extensively punctured, both when the ACB was subjected to low peak load and low frequency as also to high peak load and high frequency. However in the latter case some of the damaged portions are fairly large. The JAO sample **(Figure 11)** also exhibits extensive damage although the nature of damage does not have any bearing on the peak load and frequency. The SGT sample **(Figure 12)**, on the other hand, exhibits very large number of only pinholes surrounded by fused and darkened fabric portions.

The history of typical damages on the three types of A/O samples is listed in Table 5. It is observed from the Table 5 that the extent of crack propagation in both ACBs reinforced with the JGT samples is equal although the time (number of cycles) taken for the crack flow is much higher when the peak load and frequency are lower. The ACB reinforced with JAO sample on the other hand does not show any crack growth at all while the ACB reinforced with SGT exhibits easy growth of crack. Hence, the extent of fabric damage or the absence of

it does not have any bearing to crack growth. Moreover, it is also evident that the raw fabric strength is not decisive in preventing crack propagation as the ACBs reinforced with weaker JAO do not show any crack growth whereas those with the stronger JGT exhibit prominent reflection crack.

Role of A/O fabric in preventing growth of reflection crack

From the results of the experiments described in the fore-going, it is possible to conclude that ACBs reinforced by a grid-like A/O fabric with flexible strands perform better in preventing crack propagation as compared to sheet-like fabrics. Evidently the openings in the grid (largest grid opening size of JAO, 23 mm x 16 mm) permit the larger aggregate particles (Table 2) from the overlay to pass through the grid openings and enter suitable voids in the damaged aggregate layers below the A/O fabric. On solidifying, these particles bridge the two layers of aggregate across the fabric permitting the entire beam to behave as continuum. Moreover, such linkages across the fabric enable a better utilization of fabric strength during distortion. In the process of passing through the grid openings, some of the strands of A/O fabric do get damaged or are pushed apart. Nonetheless, the remaining load-bearing strands contribute significantly to the overall strength of the beam as evidenced by lack of any crack growth observed from the experiments conducted.

The sheet-like fabrics, whether the high-strength, low-elongation JGT or the low-strength, high-elongation SGT, did not permit proper interlocking of aggregate particles across the fabric. Some particles did puncture the JGT fabric at isolated points but could not lodge properly within the voids across, whereas the only damage experienced by the SGT fabric was due to localized melting of fibres caused by some of the hot particles of the aggregate. Consequently, the performance of both these types of A/O fabrics has been inferior to that of the grid-like fabric.

It is thus necessary to design an A/O fabric in the form of a grid in keeping with the particles size of the aggregate of the overlay so that wherever possible the particles of larger size can pass easily through the openings of the grid and from a bridge with the cracked layer below, without causing significant damage to the fabric. Hence, the pore size of the grid should be chosen keeping the larger particles of the aggregate in view.

Table 5. Exhumed sample history of different A/O fabrics.

Test conditions			Observations			
Maximum peak load (kN)	Frequency (Hz)	Type of fabric	Number of installation damages	Number of cyclic mechanical loading damages	Length of crack (mm)	Number of cycles
0.42	12	JGT	8	0	30	15786
0.78	18	JGT	12	2	30	3184
0.78	15	SGT	Innumerable	0	30	6297
0.78	15	JAO	Not distinguishable from each other		0	19865

SUMMARY AND CONCLUSION

A leno-based woven construction was chosen for devel-oping A/O fabric of moderate capability made 100% out of jute which is suitable for low traffic roads. Grab and wide-width tensile tests were performed to assess the tensile properties of the newly developed JAO.

Performance evaluation of JAO in preventing crack propagation within pavement was carried out by means of cyclic mechanical testing of dry and hygrally treated ACBs reinforced with JAO along with other two commercial A/O fabrics, i.e. JGT and SGT. The broad conclusions from the study are: (1) grab breaking strength values are much higher than those of wide-width values in terms of linear meter width. This is attributed to the difference in specimen size and test conditions, like the rate of deformation, gauge length and jaw width adopted in the two testing methods. (2) Deviation of the load-bearing standard warp threads as also the thick weft threads from their destined straight path due to tension related problems during weaving results in a consid-erable gap between targeted and achieved tensile strength and modulus of JAO. But the targeted breaking elongation value (from wide-width test) has been achieved. JAO exhibits a distribution of grid openings between small ones measuring 4 mm x 4 mm to large ones of 23 mm x 16 mm. (3) Though the strength and modulus values of JGT are higher than those of JAO, the latter performs much better in preventing crack propagation within ACB than the former under dry as well as under hygrally treated conditions. A grid-like structure of JAO helps in proper interlocking among the aggregates of the overlay and the voids of the old pavement surface below the fabric. Con-sequently, the two layers above and below the A/O fabric behave as a continuous system. On the contrary, sheet-like structure of JGT and SGT do not permit proper inter-locking across the fabric and consequently show very poor performance.

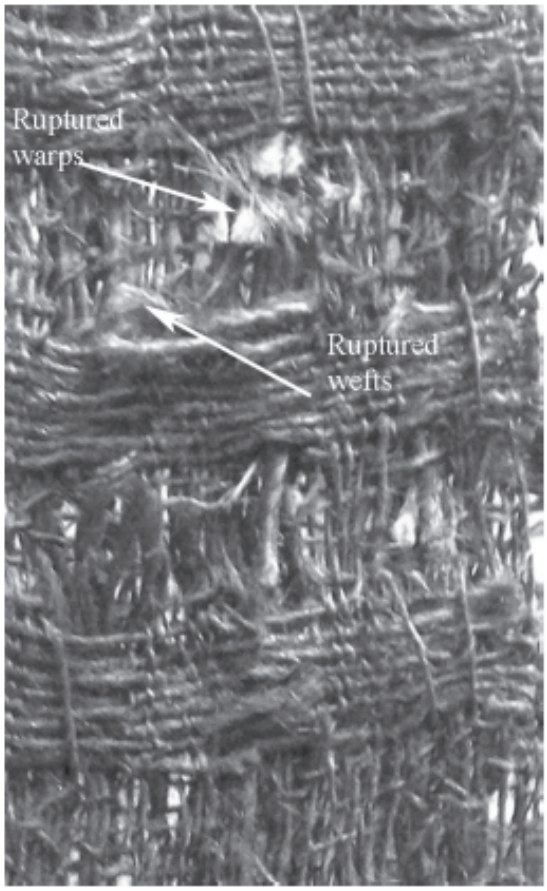

Figure 11. Exhumed JAO sample tested at maximum peak load = 0.78 kN, frequency = 15 Hz.

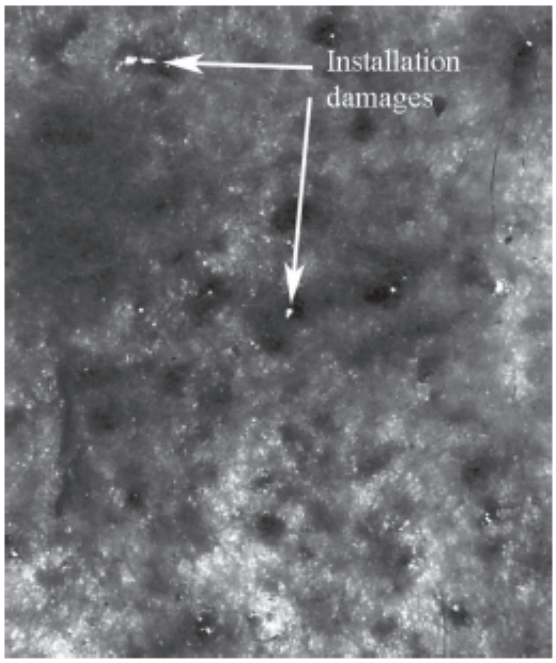

Figure 12. Exhumed SGT sample tested at maximum peak load = 0.78 kN, frequency = 15 Hz.

Additionally, the opening size of the grids of an A/O fabric should be compatible with the larger aggregates of the AC mix used in pavement so that those particles can pass easily through the openings of the grid without causing significant damage to the fabric.

Hence, the following specific conclusions can be drawn:

1. Wavy orientation of load-bearing warp and weft threads caused reduction in effective strength values in both the directions because of unequal load sharing among the threads.
2. It is not the superior tensile properties but the suit-able construction of the A/O fabric which plays main role in creating proper anchorage between overlay and old pavement surface and thereby prevents crack prop-agation into the overlay. A grid-like structure of JAO is therefore more suitable for proper interlocking than sheet-like fabric structures.
3. The opening size of the grids of an A/O fabric should be compatible with the larger aggregates of the AC mix used in pavement and plays a vital role in maintaining integrity of the overlaid pavement system through as-sistance in creating proper interlocking with minimal fabric damage.

REFERENCES

Austin, R.A., & Gilchrist, A.J.T. (1996). Geocomposite enhanced performance of asphalt pavements using geocomposites. *Geo-textiles and Geomembranes, 14(3-4),* 175-186.

Banerjee, P.K., & Ghosh, M. (2008). Studies on jute-asphalt com-posites. *Journal of Applied Polymer Science, 109(5),* 3165— 3172.

Barazone, M. (1990). Paving fabric interlayer membranes and installation procedures over the past 20 years. *Geotechnical Fabrics Report, 10(4),* 16-21.

Barry, G.F. (1985). Pavement fabrics: Do they really work? *Geotechnical Fabrics Report, 3(4),* 21-25.

Batra, S.K. (1998). Other long vegetable fibers. In M. Lewin & E.M. Pearce (Eds.), *Handbook of fiber chemistry* (Vol. 4, 2nd ed.). New York: Marcel Dekker.

Bernard, E, & Dobrosielskli, J.H. (1996). Canadian climate tests paving fabric's performance. *Geotechnical Fabrics Report, 14(3),* 30-33.

Brown, S.F., Thorn, N.H., & Sanders, P.J. (2001). A study of grid reinforced asphalt to combat reflection cracking. *Journal of the Association of Asphalt Paving Technologists, 70,*543-570.

Cho, S.-D., Kim, N.-H., Lee, D.-Y, & Kim, J.-H. (2004). A study on the performance of crack resistance for glass fiber-sheet reinforced asphalt pavement. In J.B. Shim, C. Yoo & H.-Y, Jeon (Eds.), *Proceedings of the 3rd Asian Regional Confer-ence on Geosynthetics — Now and Future of Geosynthetics in Civil Engineering* (pp. 453-462). Seoul, Korea: Korean Geosynthetics Society.

Cowell, M., Walls, J., & Salmon, L. (1985). The use of geogrids in the design of paved roads. *Geotechnical Fabrics Report, 3(4),* 28-32.

Dempsey, B.J. (2002). Development and performance of inter-layer stress-absorbing composite in asphalt concrete overlays. *Transportation Research Record: Journal of the Transporta-tion Research Board, 1809,* 175-183.

Geogrid Product Data (2002). *Geotechnical Fabrics Report, 20(9),* 157-176.

Geotextile Product Data. (2002). *Geotechnical Fabrics Report, 20(9),* 61-97.

Justo, C.E.G. (1989). Role of geosynthetics on pavement over-lays. *Application Potential of Geosynthetic Workshop,* Central Building Research Institute, Roorkee, India, 126-130.

Komatsu, T, Kikuta, H., Tuji, Y, & Muramatsu, E. (1998). Dura-bility assessment of geogrid-reinforced asphalt concrete. *Geo-textiles and Geomembranes, 16(5),* 257-271.

Lugmayr, R.G., Tschegg, E.K., & Weissenbock, J. (2002). The use of geosynthetics in paving applications - factors influencing the reflective cracking In P. Delmas, J.P., Gourc & H. Girard. (Eds.), *Proceedings of the 7th ICG on Geosynthetics: State of the Art- Recent Developments* (Vol. 3, pp. 935-938). Lisse, Netherlands: A.A. Balkema Publishers.

Lytton, R.L. (1989). Use of geotextiles for reinforcement and strain relief in asphalt concrete. *Geotextiles and Geomem-branes, 8,*217-237.

Marienfeld, M.L., & Smiley, D. (1994). Paving fabrics: the why and how-to. *Geotechnical Fabrics Report, 12(4),* 24-29.

Mather, R.R. (2005). Polyolefin fibres. In IE. Mclntyre (Ed.), *Synthetic Fibres: Nylon, Polyester, Acrylic, Polyolefin.* Cambridge: The Textile Institute, Woodhead Publishing.

Maurer, D.A., & Malasheskie, G.I (1989). Field performance of fabrics and fibers to retard reflective cracking. *Geotextiles and Geomembranes,* 5(3), 239-267.

Molenaar, A.A.A., & Nods, M. (1996). Design method for plain and geogrid reinforced overlays on cracked pavements. *Pro-ceedings of the International RILEM Conference on Reflective Cracking* (pp. 311-320). Maastricht, UK: Chapman & Hall.

Rao, G.V, Gupta, K.K., Raju, G.VS.S., Dixit, A., Sheogopal, & Deshpande, M.R. (1991). Use of geogrids in pavements. *Highway Research Bulletin, 44,* 91-117.

Roy, T., & Sur, D. (2003). *Handbook on jute* (pp. 14, 19). Kolkata: Indian Jute Industries' Research Association.

Stout, H.P. (1988). *Fibre and Yarn Quality in Jute Spinning* 2, 28.Manchester: The Textile Institute.